



**HAL**  
open science

## Grayscale lithography process study for sub $5\mu\text{m}$ microlens patterns

Chevalier Pierre, Patrick Quéméré, Charlotte Beylier, Sébastien Bérard-Bergery, Nacima Allouti, Marion Paris, Vincent Farys, Jérôme Vaillant

► **To cite this version:**

Chevalier Pierre, Patrick Quéméré, Charlotte Beylier, Sébastien Bérard-Bergery, Nacima Allouti, et al.. Grayscale lithography process study for sub  $5\mu\text{m}$  microlens patterns. Novel Patterning Technologies for Semiconductors, MEMS/NEMS, and MOEMS 2019, SPIE, Feb 2019, San Jose, United States. pp.49, 10.1117/12.2514712 . hal-04511262

**HAL Id: hal-04511262**

**<https://hal.science/hal-04511262>**

Submitted on 19 Mar 2024

**HAL** is a multi-disciplinary open access archive for the deposit and dissemination of scientific research documents, whether they are published or not. The documents may come from teaching and research institutions in France or abroad, or from public or private research centers.

L'archive ouverte pluridisciplinaire **HAL**, est destinée au dépôt et à la diffusion de documents scientifiques de niveau recherche, publiés ou non, émanant des établissements d'enseignement et de recherche français ou étrangers, des laboratoires publics ou privés.

See discussions, stats, and author profiles for this publication at: <https://www.researchgate.net/publication/332001000>

# Grayscale lithography process study for sub 5 $\mu$ m microlens patterns

Conference Paper · March 2019

DOI: 10.1117/12.2514712

CITATIONS

3

READS

148

8 authors, including:



**Nacima Allouti**

31 PUBLICATIONS 343 CITATIONS

SEE PROFILE



**Sebastien Berard-Bergery**

STMicroelectronics

26 PUBLICATIONS 121 CITATIONS

SEE PROFILE



**Patrick Quéméré**

Atomic Energy and Alternative Energies Commission

24 PUBLICATIONS 288 CITATIONS

SEE PROFILE



**R. Coquand**

Atomic Energy and Alternative Energies Commission

49 PUBLICATIONS 977 CITATIONS

SEE PROFILE

# Grayscale lithography process study for sub 5 $\mu$ m microlens patterns

Nacima Allouti <sup>a</sup>, Pierre Chevalier <sup>b</sup>, Sébastien Bérard-Bergery <sup>a</sup>, Valérie Rousset <sup>b</sup>, Benedicte Mortini <sup>b</sup>, Patrick Quéméré <sup>a</sup>, Florian Tomaso <sup>a</sup>, Rémi Coquand <sup>a</sup>

<sup>a</sup> CEA Leti, 17, avenue des Martyrs, 38040 Grenoble, France;

<sup>b</sup> STMicroelectronics, 850 rue Jean Monnet, 38926 Crolles Cedex, France

## ABSTRACT

The advance in microlithography has greatly helped the development of micro optical elements. Large array of microlenses can now be fabricated in the same fashion as manufacturing of integrated circuit at low cost and high yield [1-2].

Because microlens array requires well-defined and continuous surface relief profile, special methods are needed to supplement the normal microlithography to produce those spherical structures [3].

Various techniques have been developed, and the most widely used is multi-step photolithography with thermal resist reflow. However, the alternative grayscale photolithography technique appears to be the one as the most flexible and versatile method [4].

Indeed, this approach is a one-level lithography process enabling the development of 3D profiles in a photoresist masking layer. In addition, with the need to maintain or improve image quality at an ever-smaller pixel size, grayscale technic can offer one way to compensate the loss of the photosensitive area by achieving zero-gap microlens.

One other advantage of grayscale is the possibility to have, from a single lithography, objects of different shapes, but also at the same time of different sizes (especially heights); which is possible with classical lithography only by doing multi-patterning.

There are several options for performing grayscale lithography, for example the HEBS mask (high energy beam sensitive) which darkens under exposure to electrons. The option that has been chosen is to use a grayscale reticle, with varying chromium features densities that locally modulate the intensity of transmitted UV light. Being non-uniformly exposed, this allows the creation of a relief structure in the resist layer after development. The resist height after development depends on the intensity of the incident light, the exposure time and the contrast of the resist. So contrary to conventional lithography where the goal is to achieve straight resist pattern profiles, grayscale lithography enables the realization of progressive profiles, which requires smooth resist contrast curve. The other specificity of these resists is that they must crosslink without flowing.

In this paper, we evaluate resists from different suppliers to generate microlenses smaller than 5 $\mu$ m via a grayscale mask. The study consists in establishing the contrast curves of these resists according to different process parameters, giving the designer great control of grayscale levels that can be achieved for a given resist. Then, pattern various microlenses shapes in these resists to evaluate the residual resist thickness according to the gray levels. With the final objective of establishing a relationship between these contrast curves and the profile variations at the microlens level to compute a suitable and accurate grayscale mask [5].

**Keywords:** Grayscale, photo mask, micro-lens, contrast curve, photo-resist

## 1. INTRODUCTION

Microlens arrays are widely used in CMOS image sensors as light collectors. As pixels shrunk considerably in recent years, microlenses introduction significantly increased the light gathering capabilities of small pixels, effectively increasing the pixel fill factor. Indeed, if the position and the curvature of the microlens above the pixel are chosen correctly, the loss of sensitivity induced by the reduction of the photoactive area is then compensated thanks to the microlens which recover the rays of light which would normally touch the zones of the pixel that are not able to create a photo current and focus it on areas that can benefit, thereby increasing the electrical signal.

Conventional photolithography method to fabricate complex 3-dimensional structures like microlenses is to use a binary photomask, allowing creation of two-dimensional (2D) patterns in the photoresist, but with uniform height. Advanced CMOS image sensor applications require sometimes the integration of multiple microlenses presenting different height or curvature. This three-dimensional (3D) fabrication normally requires multiple photolithography and alignment processes, which are both time consuming and technically challenging. Considering this, grayscale lithography mask is a very interesting option, allowing faster production, 3D micro device prototyping.

In standard lithography, a “binary” behavior of the photoresists is desired: the exposed resist has to be completely cleared during development, while the remaining resist features should have a rectangular cross-section with steep sidewalls.

The goal in grayscale lithography is to transfer gradients of the exposure dose into a certain resist topography during development. Two types of masks are commonly used in grayscale lithography, which include halftone chromium masks and high-energy beam-sensitive (HEBS) glass masks. HEBS masks are made of specific glass that turns dark instantaneously upon exposure to an electron beam; the more electron dosage (current  $\times$  dwell time), the darker the glass gets. Halftone masks are essentially binary chromium masks that are subdivided into cells, each of which has a certain transmission value [6].

In this study, it has been chosen to use halftoning grayscale technique to evaluate resist from different suppliers to generate submicron microlenses. The generation of 3D structures having micrometer-sized features requires careful construction of the sharp gradient of gray levels at the micrometer scale on the mask.

First, briefly we will explain how grayscale mask code has been set-up for this evaluation. Then the experimental conditions and resist requirements for grayscale lithography are reviewed. Finally, in order to make the grayscale process useful for manufacturing of semiconductor devices, this paper consider the inherent process variability by studying different type of resist.

## 2. CODING GRAYSCALE MASK

The grayscale mask, used in this study was modeled by the computational lithography [7]; it is a pixelated mask, with arrays of chromium squares with different sizes at a fixed pitch; which modulate the light intensity that passes through them (Figure 1). These squares are all smaller than the minimum stepper resolution so that none is directly printed as such in the resist after development. The pitch considered for the realization of this test mask is 200 nm, lower than the resolution of an I-line stepper (250 nm). It is the size of the pitch (periodicity of the pixel matrix) as well as the size of the chromium patterns on the mask that allows this sub-resolution.

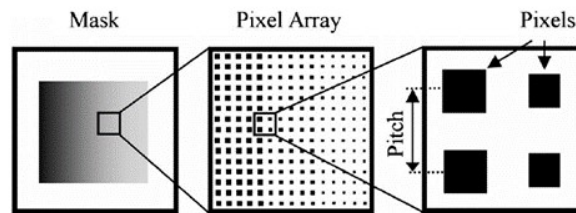


Figure 1. Zoom on a pixelated grayscale mask

The key to predict the remaining resist thickness after insolation is to be able to relate the residual resist height to the actual dose received; that is to say at a given chromium density present on the mask. This can be done by analyzing the contrast curve. For this, 51 rectangles with increasing chromium densities were embedded on the mask.

After exposure, these areas should normally give rise to 'pillars', the height of which, different for each, will gradually increase (Figure 2). The possible range of chromium densities for the pillars designed on the mask is further limited by the constraints related to the mask manufacturing, given by the supplier: on one side the size of the smallest plot of chromium achievable, and on the other the size of the smallest space achievable between two neighboring chromium patterns. In our case, the minimum Critical Dimension happens to be 40nm and the minimum Space 30nm at 1X scale (so respectively, 160nm and 120nm at mask level). The unitized pixelization grid used being 200nm apart, this implies a 170nm CDmax.

The Figure 2 below illustrates how, depending on the increasing chromium squares, as density reduces the transmitted light, the contrast curve can be traced.

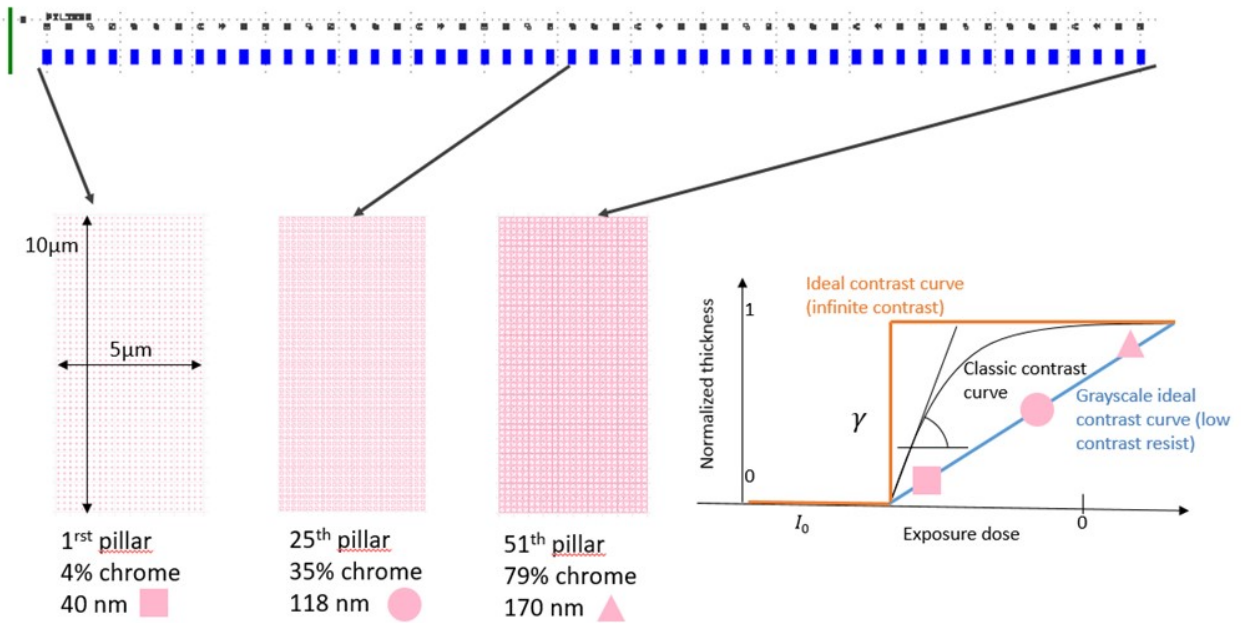


Figure 2. Correspondence between pixelization of three pillars array with different chromium densities on the mask and the resist contrast curve

Contrast curves can follow several trends, which are then approximated by mathematical functions. The behavior of the resists not being known at the start of the project, the mask data-preparation before study was executed while considering as working hypothesis a theoretical contrast curve strictly linear. From a practical point of view, the grayscale resists must have a low contrast. For this study, we seek to identify the resist that will resolve as many pillars as possible. That is to say, that will cover the most possible gray levels. The final objective of this project is to form microlenses using grayscale, so various shapes including lenses have been included in the mask too. All these forms are created to study the response of the resists to the grayscale. In this paper, we focused on dense microlens array. Figure 3 illustrates the pixelization of the mask at the level of the lens matrix. The diameter of the microlenses of interest is  $2.8\mu\text{m}$ , separated by  $400\text{nm}$ , corresponding to the pixel size for the desired technological application.

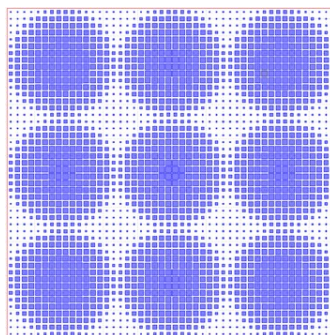


Figure 3. Example of dense microlenses pixelization

### 3. RESIST REQUIREMENTS FOR GRAYSCALE AND EXPERIMENTAL CONDITIONS

#### 3.1 Resist requirements for grayscale lithography

The optical properties (e.g., focal length) of the microlenses used in CMOS Imagers were determined first by the thickness of the photoresist and the size of the circular patterns. The control of these parameters are directly linked to resist thermal stability. This means that once the microlenses are formed, hard bake is needed to stabilize the shape. Indeed, contrary to reflow method, with grayscale technic the key process parameter is to have “non-flow” of resist material. To have resist cross-linking without melting, we need to work ideally with resists whose glass transition temperature  $T_g$  is higher than the crosslinking temperature.

Moreover, as previously explained for grayscale mask preparation, it is critical to have resist material with low contrast transition, with a response versus dose as smooth as possible.

For standard I-line positive resists with thickness less than  $2\mu\text{m}$ , the penetration depth of light is higher than the resist film thickness. Hereby the resist film is exposed almost homogeneously from the surface towards the substrate from the very beginning of exposure, so it is not possible to attain a vertical exposure dose profile in the resist film. Therefore, the only mechanism which allows grayscale lithography is the dependency of the development rate from the exposure dose. However, resists are generally optimized for high contrast. This means that they (almost) do not develop below a certain minimum exposure dose, and develop at a constant rate from a higher exposure dose on (black curve in Figure 2). Since both doses are close from each other, there is only a small exposure dose window in which one can adjust the development rate. In order to make the process more reproducible, it is possible to spread the curve towards an almost linear dependency between exposure dose and development rate. This can be attained via different process parameters possible adjustments. First we can reduce or increase post-apply bake process (also called a softbake or a prebake), which keeps the concentration of the remaining solvent high, thus increasing the dark erosion in the developer and hereby lowering the contrast. Alternatively, a hot or long softbake decomposes a significant part of the photoactive compound DNQ, thus reducing the development rate and increasing the dark erosion at the same time, (unexposed DNQ is a development inhibitor). Additionally, a short flood exposure will cause an offset in the development rate. Finally, a high developer concentration can lower the selectivity of the developer, which is equivalent to a lower contrast. All these process key parameters have been investigated.

In this study, experiments were carried out using two “under-development” on non-commercially I-line photosensitive positive resist called Polymer A and Polymer B (see Table1). Both material has been recommended by suppliers as low contrast resist; even though they both contain Diazo NaphtoQuinone (DNQ) which by default makes them more absorbent.

Item	Resist A	Resist B
Photo-sensitivity	Positive	Positive
Chemistry base	Acrylic + DNQ	Polymer + DNQ
Thickness range	[0,9 ; 1,4] $\mu\text{m}$	[1,1 ; 1,8] $\mu\text{m}$
Measured $T_g$	[75;85] degrees	[50;55] degrees
Cross-linking $T^\circ\text{C}$	[139;151] degrees	[148;152] degrees
Pre-Bake	90°C-90s	90°C-90s
Development	TMAH 1,2% 60s	TMAH 1% 60s
Post-Bakes	Bake1:140°C-300s Bake2:150°C-300s	Bake1:160°C-300s Bake2:180°C-300s

Table 1. Resist A and resist B properties

We see from the beginning that none of the two ideal conditions for a “good grayscale lithography” is met with the tow selected resists under evaluation. Neither condition 1, which means having a  $T_g$  lower than the crosslinking temperature to avoid resisting melting; neither really condition 2, that is to say having a true "low contrast" resist, is respected. Nevertheless, based on the materials currently available on the market, we have studied the inherent process variability of grayscale lithography in order to guide the development of the best material formulation in the future.

### 3.2 Experimental conditions

The sample preparation and evaluation were conducted as follows: lithography stack is initially composed of two sub-layers: one anti-reflective (BARC: Bottom Anti-Reflective Coating) and the other known as planarization, both directly spin-coated on 12-inch silicon wafers. The spread of the resist of interest is then carried out by spin coating too with soft baked at 90°C during 90s for both resist.



Figure 4. Diagram of resists stack for grayscale lithography

Then wafers were exposed on an I-Line stepper (NA=0, 57;  $\sigma=0, 70$ ) and developed in a basic aqueous solution for 60s.

The final step of the process consists in stabilizing the grayscale microstructure transferred into the resist by crosslinking through annealing of the resist. In order to prevent resist reflow during these cross-linking bakes, treatments or specific conditions will be studied and evaluated.

The fabricated “pillar” structures remaining thickness used to build calibration curves were acquired using a high-resolution profilometer (HRP340A from KLA Tencor). In addition, microlens dimension, top views and shape was observed respectively through critical dimension scanning electron microscope (CD-SEM Verity4i+ and SEMVision G3 from Applied Materials) and a 3D Atomic Force Microscopy (AFM 3D Insight3D from Bruker).

## 4. LITHOGRAPHY PROCESS WINDOW WITH GRAYSCALE MASK

### 4.1 Lithography performances

As standard lithography, first step was to investigate the resist performances. For that we determine the lithography process window, which is typically defined as the set of {focus, exposure} points to control critical dimension (CD) variation to within 10%. One simple way visualizing it is using a Focus-Exposure Matrix (FEM) curve which plots exposure vs. defocus for a given linewidth tolerance. Maximal inscribed rectangle in this plot then represents the process window. Best process is generally the one that varies the least and offers the largest window. This also applies to grayscale lithography, especially since this will allow us to determine the dose sensitivity of the resist, an essential parameter for the grayscale application. So for a CD Target of  $2.8\mu\text{m} \pm 10\%$ , process window for each resist under evaluation are reported in Figure5. FEM were performed for doses between 800 and 2600J/m<sup>2</sup>, focus from -0.9 to +0.9µm. The main effect on the lens size for both resists is dose and both process windows are quite large and comparable. Even though we can observe a slight difference between dose sensitivities, indeed Resist B is more sensitive than Resist A with respectively a dose sensitivity of  $\sim 3\text{mJ}/\text{nm}$  compare to  $\sim 2\text{mJ}/\text{nm}$ .

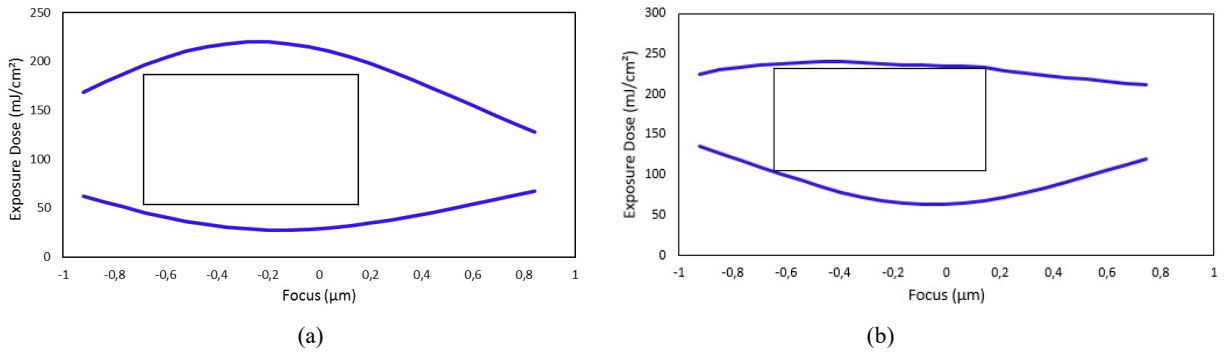


Figure 5. Process window of Resist A (5a) and Resist B (5b)

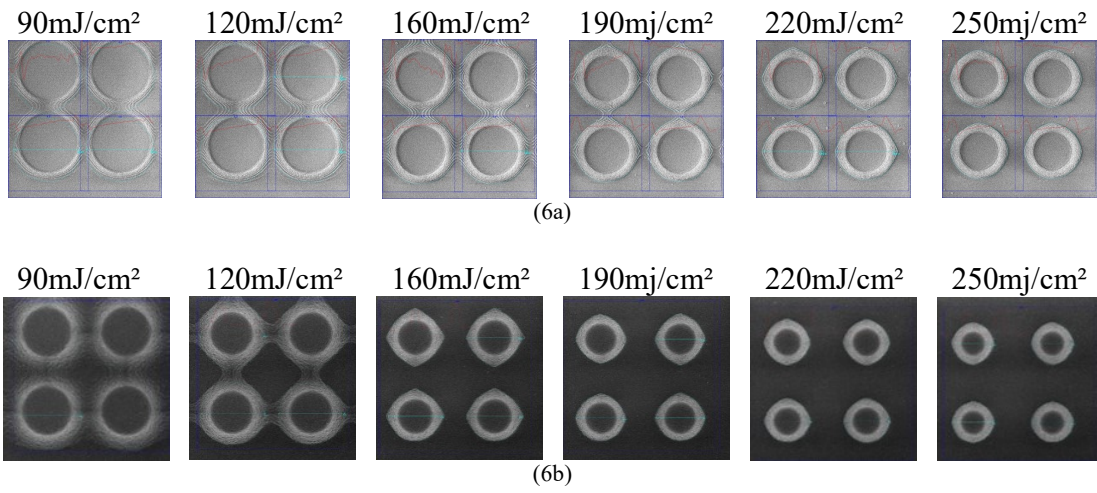


Figure 6. Effect of exposure dose on 2.8μm micro lenses shape on resist A (6a) and Resist B (6b)

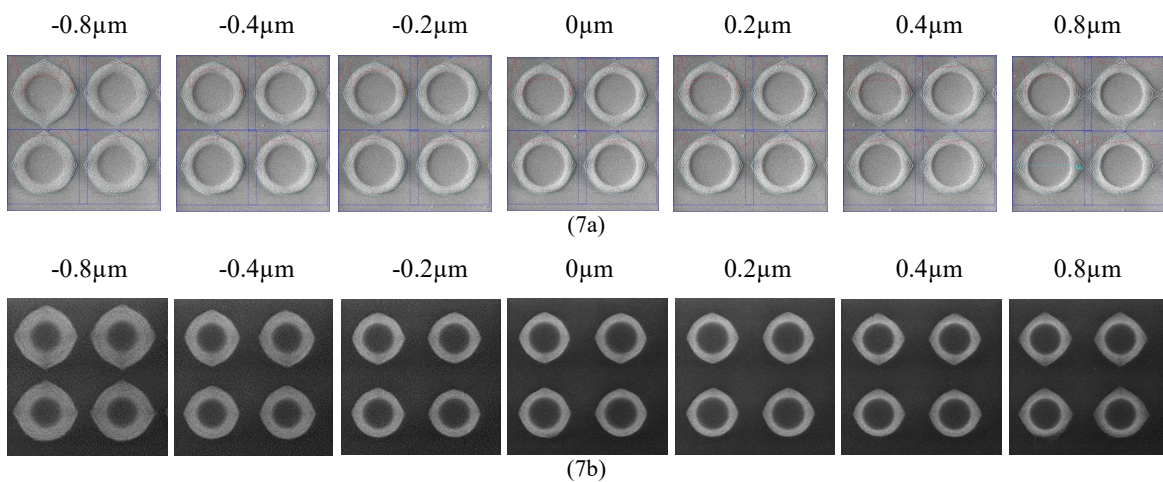


Figure 7. Effect of exposure focus on 2.8μm micro lenses shape on resist A (7a) and Resist B (7b)

## 4.2 Resist contrast curves

On same FEM, we used a profilometer to measure the height of the resulting 51 pillars in each resist for different doses and focus. The contrast curves for different doses and focus for Resist A (8a) and Resist B (8b) are depicted in Figure 8. Both resist differentiate from each other by the shape of their contrast curves; but they both cover almost the same range of gray levels, indeed both solve same pillars range for a given process set point.

As with the FEMs previously, the effect of the dose is important: the number of pillars depends on it. As expected following grayscale mask design; the higher the dose, the fewer the pillars. Same focus has a second order effect but does not have a clear trend.

Moreover, Resist B has a steeper slope than A, which corresponds to a higher sensitivity dose, already observed in the analysis of the process window. The translation following the dose of the contrast curves for the resist A seems more progressive and smooth than for the Resist B. Based on the sensitivity dose, it may be possible to obtain less range of doses available given for a finite number of gray levels with the Resist B.

These graphs also illustrate that for each dose focus pair, we obtain a different contrast curve. This suggests what will happen if we change on process condition like pre-bake temperature or developer concentration.

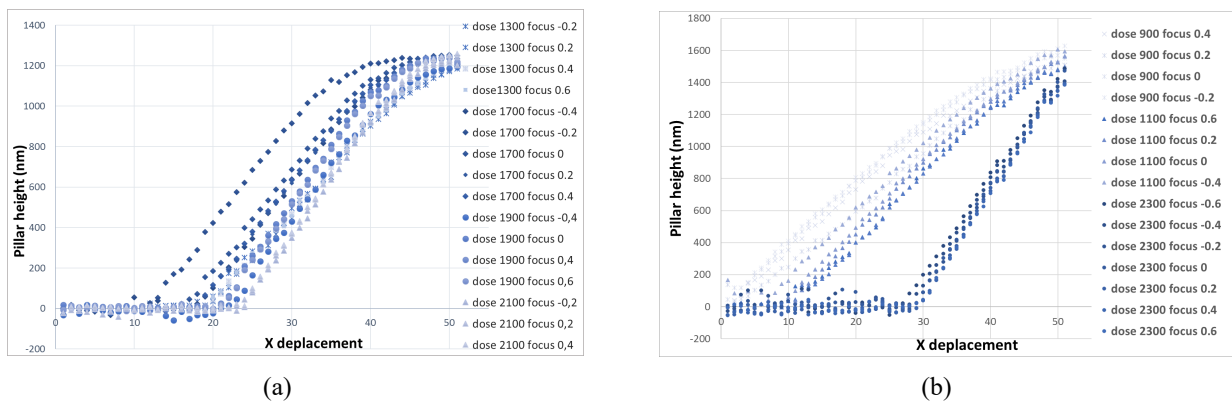


Figure 8. Resist A (8a) and Resist B (8b) contrast curves at different doses and focus

We can notice that at the end of each contrast curve, we reach a plateau anyway: there is a density of chromium beyond which the resist does not see anything. This is more visible for resist A. Therefore, we do not have totally 51 gray levels usable; but from one curve to another, we see the same trend. This may be due to the resist material itself; indeed beyond a certain dose exposure (that is to say chromium density), the threshold intensity sufficient to make a reaction of resist dissolution by the developer is not reached. For resist B, another phenomenon is also observed; as it is more sensitive resist; at higher doses the level of pillars with low densities are completely dissolved in the developer.

The comparison of contrast curves according to each resist brings us the same information concerning the dose sensitivity. With more information about the dependence of the development rate versus exposure dose. Thus, the resist analysis of the contrast curves is complementary to that of their process window.

Based from these resist performances it's not yet possible to conclude which one of the two resist is the best for grayscale lithography. Although, these experimental contrast curves pointed out intrinsic material limitation, which should have to be take into account in next grayscale mask preparation.

## 4.3 Microlenses process latitude

Final objective of this study is to form microlenses using the grayscale. The mask in grayscale was calculated by considering as theoretical working hypothesis a strictly linear contrast curve. Based on that, we observed the spherical microlenses coded with the halftoning algorithm that fit theoretical contrast curves. SEMVision tilted view of these microlenses are displayed in Figure 9(a) with resist A and 9(b) for resist B. As we can see, nice and repeatable

microlenses are obtained after development for both resist. As expected, the two resists do not respond in the same way to the same mask pixelated information.

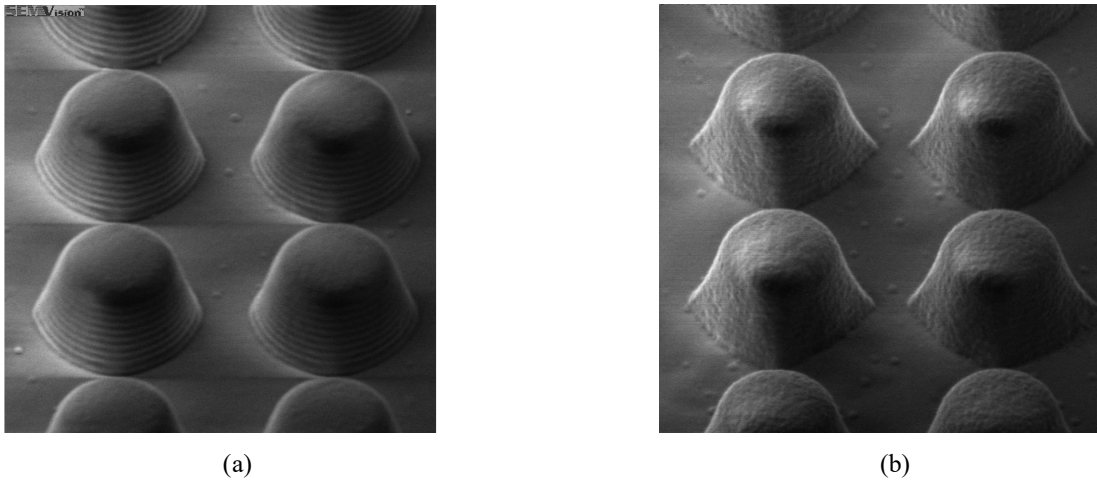


Figure 9. Resist A (9a) and Resist B (9b) SEMVision tilted view of 2.8 μm spherical dense microlenses

In the same way that a strong effect of the dose is observed on the contrast curves, this same effect is also noticed on the shape of the lenses; while the focus effect is negligible. Figure 10 shows that microlens shape evolution as a function of dose and focus for resist A (10a) and resist B (10b).

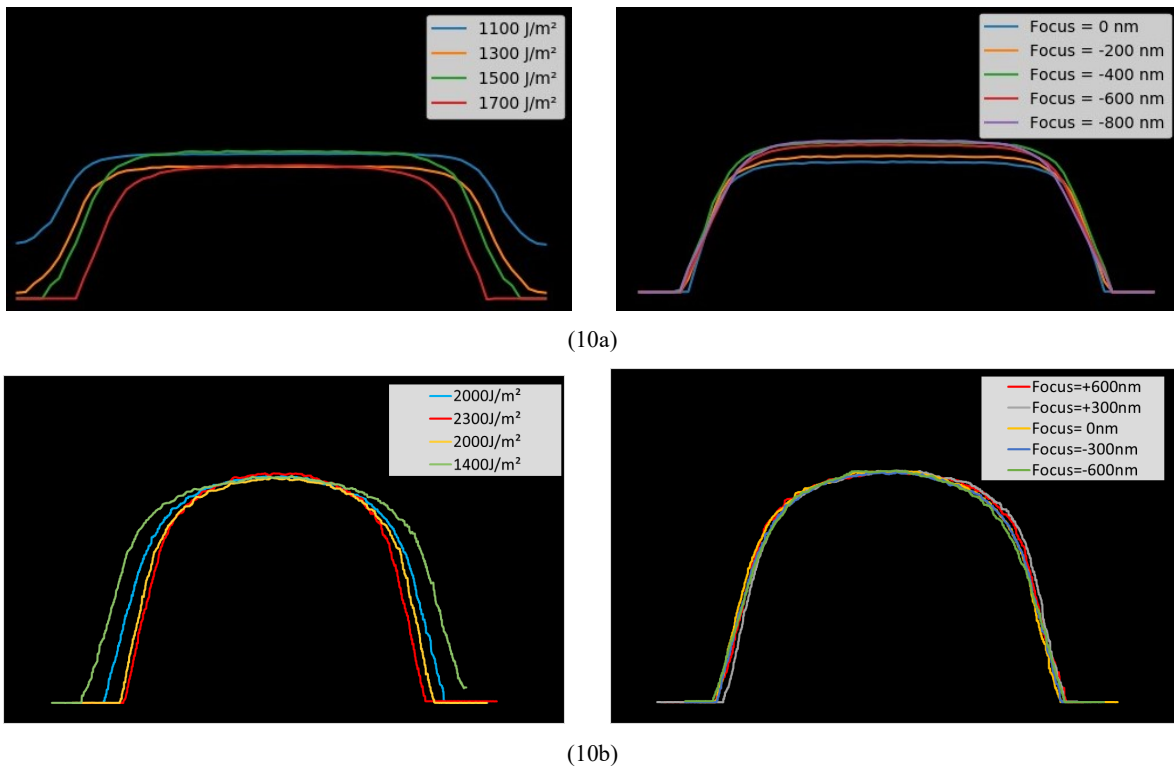


Figure 10: Comparison of AFM profiles of 2.8 μm dense microlens shape evolution as function of dose and focus for Resist A (10a) and Resist B (10b)

We have mentioned earlier the importance for grayscale lithography, to obtain a nearly linear dependence curve between the exposure dose and the rate of development. This can be achieved through different process parameter adjustments. In this study, although different process parameters have been studied, we decided to focus on softbake whose effect on the photosensitive component DNQ is not without consequence normally. A hot or long softbake breaks down a large portion of the DNQ photoactive compound, thereby reducing the rate of development and increasing dark erosion at the same time.

The study of pre-bake effect was made through a small Designed plan of experiments. Among the different experimental designs, factorial designs are common because they are the simplest to implement and they allow highlighting very quickly the existence of interactions between factors. Therefore, with two factors studied, post-bake temperature and time, this led to a minimum of five tests with a central point, to compare with the reference conditions which are 90°C during 90s for both resist A and B.

The basic assumption is to assign each factor (normalized) at its lowest value (-1) and its highest value (+1). Thus, for k factors, we end up with a set of  $2^k$  possible values. The Table 2 details the experimental conditions of the experimental design: two levels per factor plus a central point.

	Configuration	Factor1 Post-Bake Temperature (°C)	Factor 2 Post-Bake time (seconds)
Test1	--	90	60
Test2	--+	90	120
Test3	+--	110	60
Test4	++	110	120
Test5	0	100	90
Reference		90	90

Table 2. Design of experiments plan

The result of each test is expressed by the contrast curve that covers the largest number of pillars. As we have seen that dose, sensitivity can be correlated to contrast curve, so we have also measured this parameter as a second response. In this case, it is considered that the slope of the contrast curve will be representative of the dose sensitivity. The tests were done and the results are summarized in the following Table3:

	Best process conditions Dose mJ/cm <sup>2</sup> / Focus μm	Number of pillars covered	Dose sensitivity
Test1	110 / -0,6	51	32,9
Test2	110 / +0,2	51	37,2
Test3	130 / +0,4	51	36,9
Test4	130 / +0,2	51	33,9
Test5	130 / +0,8	51	35,6
Reference	110 / -0,5	51	33,0

Table 3. Design of experiments results

As before, for each of the test, a matrix exposure dose was realized. Each of the wafers was then measured using a profilometer in the same manner as the reference wafer. This leads to obtain, for each test, 68 contrast curves for dose / focus pairs of between [900; 2500] J/m<sup>2</sup> and [-0.8; 0.8] μm. The analysis of these curves allows selecting that which covers the maximum of pillars. Finally, for each of the five tests, a contrast curve with the 51 pillars fully resolved was found for different dose/focus conditions. These contrast curves for Resist A are plotted in Figure 11. In addition, for each of these five contrast curves, the slope has been calculated. Regardless of the test, the difference between each of the contract curves compared to the reference contrast curve made following the supplier recommendations is not significant. Same, none of the tests carried out shows a better dose sensitivity than the one obtained with the reference. Moreover, we obtained almost same behavior for Resist B regarding pre-bake conditions effect. The field of study chosen to vary the conditions of the annealing post application bake was perhaps not sufficiently extended. Or maybe the pre-bake has no significant effect on the contrast curve. In any case, a pair of optimized conditions dose/focus makes it possible to solve the same amount of gray levels for each resist.

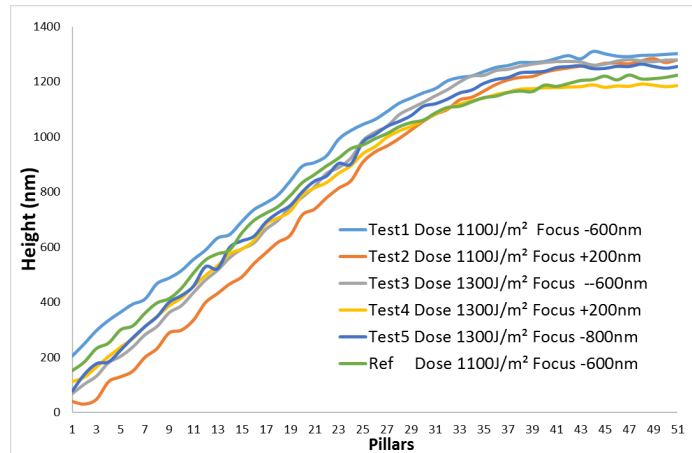


Figure 11: Design of experiments contrast curves results, best process conditions for each test performed with Resist A

This design of experiment outlines the fact that process parameters like pre-bake temperature or time do not significantly affect the resist contrast curve of the two selected resists; the global shape is conserved and an operating point may be found to get the resolution of the maximum gray levels pixelized on the mask.

## 5. HARDBAKE CONTROL POST GRAYSCALE LITHOGRAPHY

As explained before, one specific requirement associated to grayscale lithography is the use of non-reflow microlens resist type. Indeed all the work done at the level of mask modeling to transfer the 3D form in the resist must not in any case be modified during the crosslinking bake steps. Although as mentioned before, the two selected resists for this evaluation have not their crosslinking temperature under their  $T_g$ ; so at least one important thing is to minimize the change of microlens shape.

For each resist, the aim was first to optimize annealing steps to avoid resist melting. Depending on the resist, we obtained very different results.

### 5.1 Resist A reflow behavior

For Resist A, supplier recommend to perform a first bake at 140°C and a 2<sup>nd</sup> bake at 150°C during 5min each. Following their recommendations, we clearly noticed that melting occurs during the hard bake step, which significantly changes the microlens shape, and this already from the first annealing at 140 °C. Indeed, we see in Figure12 (e), that during the first bake the microlenses merge.

To avoid resist melting, we investigate different hard bake temperature starting from 110°C to 150°C, to determine the “non-flow” window temperature range of Resist A. We noticed that the temperature range with limited resist flow is quite small, namely between 110°C and 120°C. By optimizing the hard bake, temperature steps it is possible to reduce resist melting.

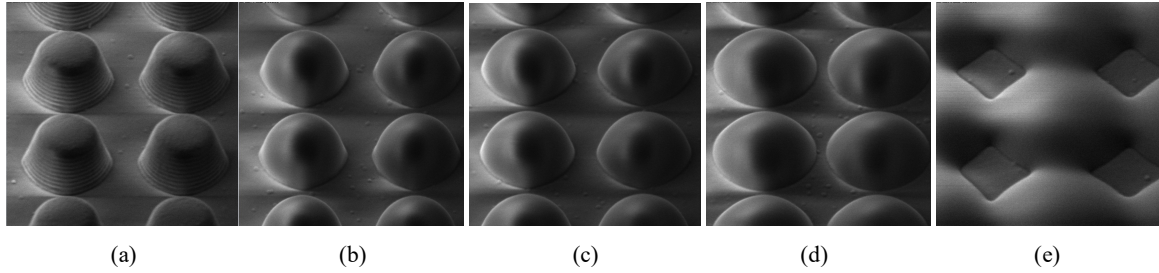


Figure 12: Comparison of SEMVision tilted view of microlens obtained after development (a) after Bake 110°C-5min (b) after Bake 120°C-5min (c) after Bake 130°C-5min (d) and after Bake 140°C-5min (e)

In Figure 13, we see that with two consecutive bakes of 110°C and 120°C during 5min each, before the first recommended hard-bake at 140 °C; the microlens shape is best preserved. However, at least third consecutive bakes are required for this resist, which is quite time consuming, thus not compatible with an industrial process. In addition, whatever the bakes sequence the initial shape after grayscale lithography is modified with huge height shrink (see Figure 14), which is not complying with grayscale requirement.

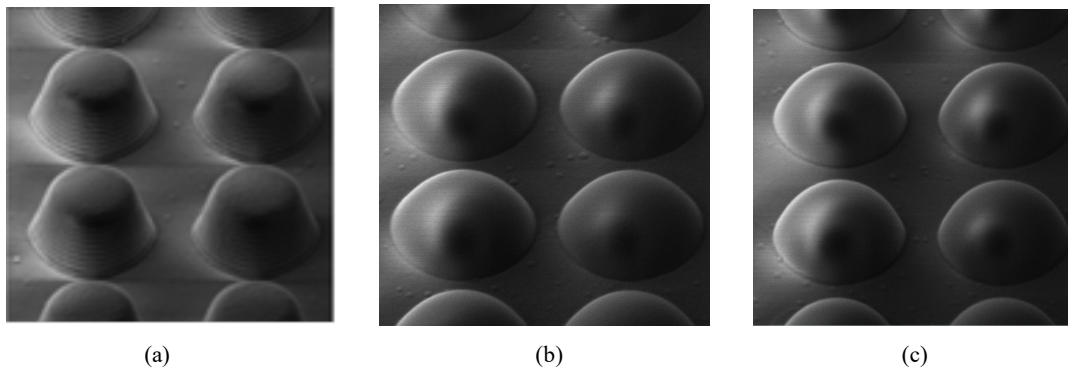


Figure 13: Comparison of SEMVision tilted view of microlens obtained after development (a) after three consecutive bakes: Bake1 120°C-5min + Bake2 140°C-5min + Bake3 150°C-5min (b) and after four bakes: Bake1 110°C-5min+Bake2 120°C-50mmin + Bake3 140°C-5min + Bake4 150°C-5min (c)

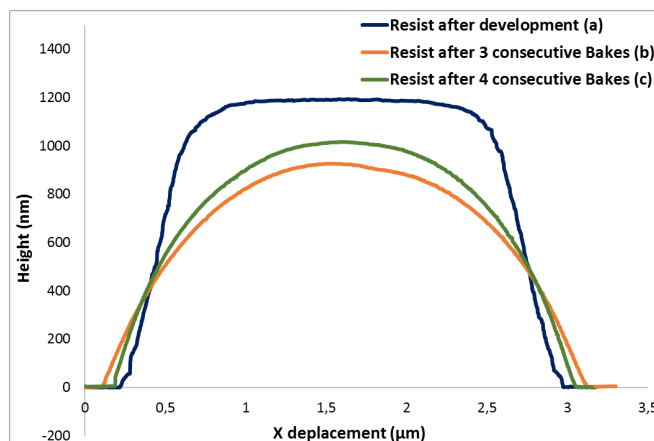


Figure 14: AFM profiles of 2.8µm dense microlens shape obtained after development compare with two different baking sequence

## 5.2 Resist B reflow behavior

For Resist B, we apply same method. First, we check resist reflow behavior in supplier recommended hard-bakes conditions, which are 1st bake at 160°C and a 2nd bake at 180°C during 5min each. In that case, although we have also a slight melt of the microlens after 1st bake just after development compare to initial shape; we have no merge of the microlenses (see Figure 15). This is certainly, because resist B Tg's is higher and closer to its cross-linking temperature than Resist A, hence the process of cross-linking is initiated faster.

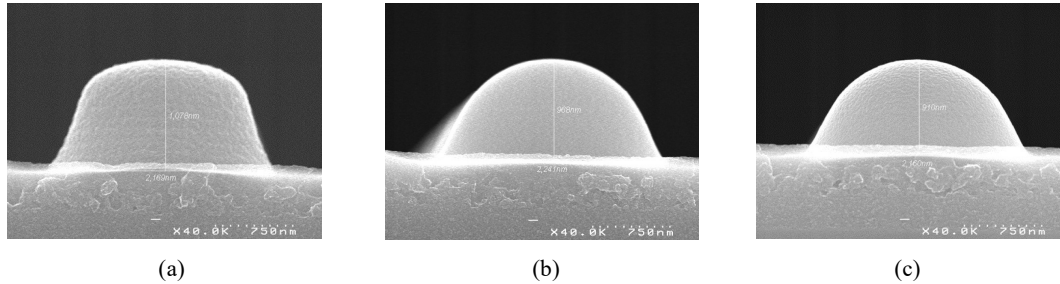


Figure 15: Comparison of MEB cross section view of microlens obtained after development (a) after Bake1 160°C-5min (b) and after two consecutive bakes: Bake1 160°C-5min + Bake2 180°C-5min (c) for Resist B

As reported below on Figure 16; by introducing a previous bake at 120°C during 5min we observe no big gain on resist profile change; compare to recommended bakes sequence conditions. Whatever the sequence conditions, we observe that the profile is slightly modified especially at the level of the resist top.

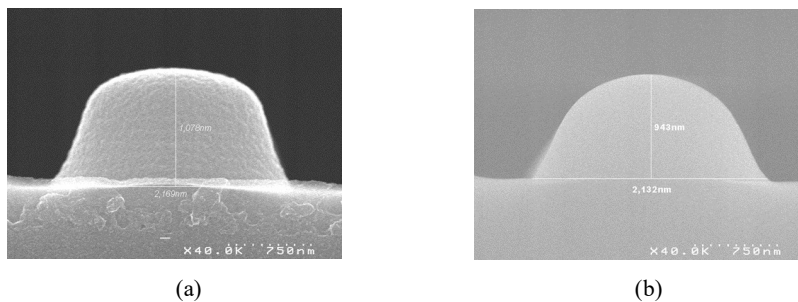


Figure 16: Comparison of MEB cross section view of microlens obtained after development (a) after three consecutive bakes: Bake1 120°C-5min + Bake2 160°C-5min + Bake3 180°C-5min (b) for Resist B

These results are confirmed by AFM profiles measurement, which are displayed on Figure 17 below.

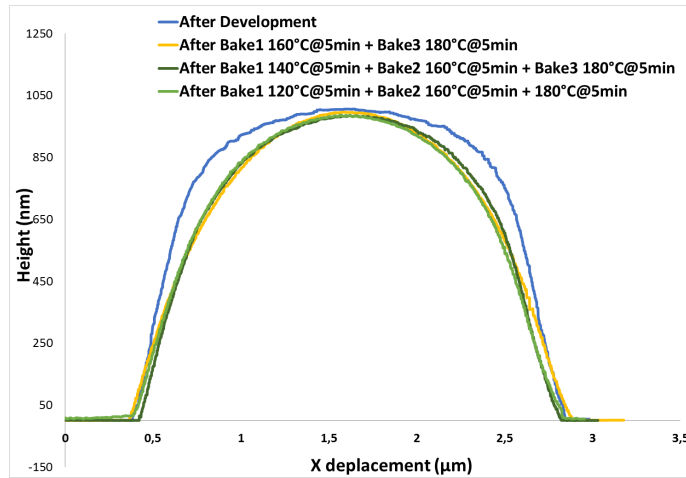


Figure 17: Comparison of AFM 3D microlens profiles obtained after development compare with two different baking sequence

Other tests to freeze the shape of the microlens immediately after development were tested too. Like adding an exposure step on microlenses already formed after development and before annealing steps. The idea is to see if, under the effect of UV exposure or "bleaching", the resist will sufficiently cross-link at the surface to avoid this type of melt afterwards. For the two resists, this additional step was ineffective, even at high dose (see Figure 18).

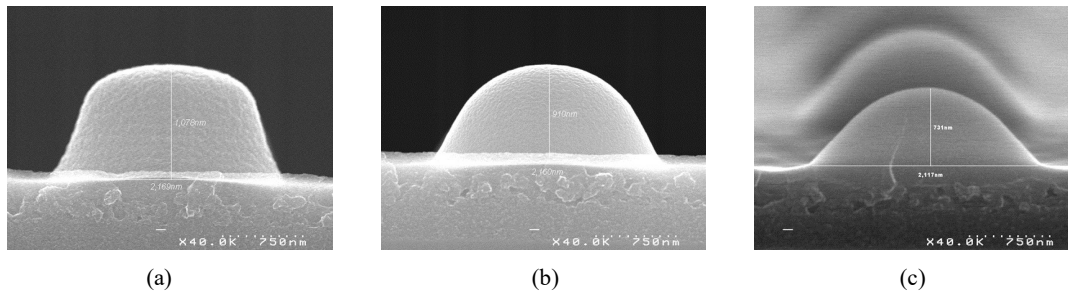


Figure 18: Comparison of MEB cross section view of microlens obtained after development (a) after Bleaching step 800mj/cm<sup>2</sup> wavelength 365nm (b) after Bleaching step 800mj/cm<sup>2</sup> wavelength 157nm (c) for Resist B

Likewise, other attempts under particular annealing conditions have been evaluated (see Figure 19). Based on the assumption that oxygen enters the resist reflow mechanism or participate to crosslinking kinetics. We have performed first bake step at 160°C under nitrogen with less than 100 ppm of oxygen; It was observed that in a annealing with limited O<sub>2</sub>, the resist does not flow anymore. Then if on same wafer, we finalize the crosslinking processus with the second bake at 180°C during 5min under atmospheric pressure; the microlens shape is almost preserved as illustrated on Figure 19(c). This has been also confirmed by AFM measurements on Figure 20.

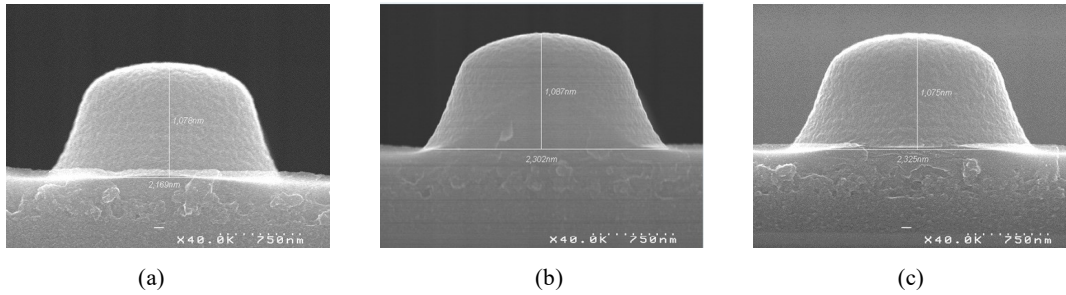


Figure 19: Comparison of MEB cross section views of microlens obtained after development (a) after Bake1 160°C-5min under O<sub>2</sub> <100ppm (b) after Bake1 160°C-5min under O<sub>2</sub> <100ppm + standard Bake2 180°C-5min under atmospheric air (c) for Resist B

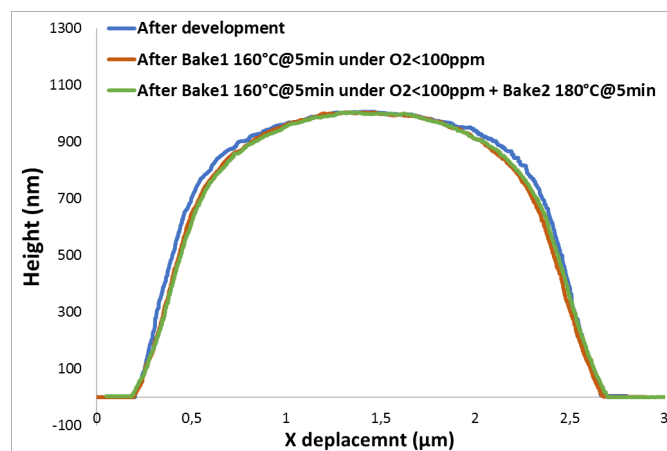


Figure 20: Comparison of AFM 3D microlens profiles obtained after development compare to bakes sequence with Bake1 160°C@5min under O<sub>2</sub><100ppm for Resist B

Thermal analysis and other tests are in progress to confirm that with the introduction of this annealing step under O<sub>2</sub> <100ppm; the resist is correctly cured at the end. In addition, more accurately, we will study the effects on various shapes and sizes of microlenses.

Finally, for Resist B we manage to find a baking sequence, which has minimum impact on grayscale lithography shape but which is not without effect either. This means that in grayscale mask computing, this variable may also has to be considered.

## 6. CONCLUSION AND PERSPECTIVES

In this study we have shown that starting from a grayscale mask based on a theoretical model of a linear contrast curve, we obtained from two different positive tone resists the expected sub-5μm microlens shape thus pixelated on the mask. Moreover, for each of the two resists under evaluation assimilated as "low contrast" resist, we found a process point able to solve same levels of gray.

From lithography process point of view, the two resists under evaluation exhibit almost same performances; with a quiet and comfortable process window for a CD target at 2.8 $\mu\text{m}$ . Apart dose sensitivity which is slightly higher for Resist B than Resist A; no process element makes it possible to say that one is better than the other.

The study of the reflow process window during crosslinking bakes has allowed distinguishing the resists from each other. Indeed, despite attempts to optimize cure conditions, it was not possible to avoid Resist A melting during hard bake steps without modifying microlense shape. Whereas for Resist B, a set point has been found, which permit to keep the microlens shape formed after lithography development during crosslinking bakes. Even for Resist B, it will be necessary to consider in the mask model this reflow variable although minimal. Especially if we considered that this process point thus found may be different depending on other microlenses dimensions and forms.

This works highlights the limitations of low contract resist now available on the market for grayscale applications. The challenge does not ultimately lie in the objective of having the most low-contrast material possible but rather to find a formulation that can be used to crosslink quickly enough to preserve the benefit of all the mask coding work. Otherwise, it will be necessary to provide in addition the reflow simulation according to a given resist for grayscale model.

## REFERENCES

- [1] Stefan Sinzinger, Jurgen Jajms, Wiley, Micro optics 2nd Edition, ISBN: 3-527-40355-8 (2002),
- [2] Nock, V. & Blaikie, R. J., 'Fabrication of optical grayscale masks for tapered microfluidic devices', *Microelectronic Engineering* (2008)
- [3] Audran, S.; Vaillant, J.; Farys, V, 'Grayscale lithography process study applied to zero-gap microlenses for sub 2 $\mu\text{m}$  CMOS image sensors', *Proceedings of SPIE* (2010)
- [4] Zheng C.; Jinglei Du b; Yongkang G., 'Overview of Greyscale Photolithography for Micro optical Elements Fabrication', *Proceedings of SPIE* (2003)
- [5] Gan, O.; Allen, P.; Barkai, A., Programmed resist sidewall profiles using subresolution binary grayscale masks for Si-photonics applications, *Advanced Fabrication Technologies for Micro/Nano Optics and Photonics V* (2012)
- [6] Su, J., Du, J., Yao, J., Gao, F., Guo, Y. and Cui, Z., 'A new method to design half-tone mask for the fabrication of continuous micro relief structure', *Proceedings of SPIE* 3680(1999)
- [7]Chevalier P.; Quéméré P.; Beylier C.; 'Beyond contrast curve approach: a grayscale model applied to sub 5 $\mu\text{m}$  patterns', *Proceedings of SPIE* (2019)